

## Mesoscopic Modeling of Slip Motion at Fluid-Solid Interfaces with Heterogeneous Catalysis

Sauro Succi

*Istituto Applicazioni Calcolo, CNR, V.le del Policlinico 137, 00161, Roma, Italy*

(Received 27 November 2001; published 19 July 2002)

The onset of slip motion at fluid-solid boundaries is investigated as a function of the reflectivity of the solid wall by means of a mesoscopic lattice Boltzmann model. Substantial slip flow is observed for reflectivity values below a critical threshold. It is shown that this slip flow may significantly affect the conversion efficiency of catalytic microchannels.

DOI: 10.1103/PhysRevLett.89.064502

PACS numbers: 47.15.-x, 67.40.Hf, 82.45.Jn

A deeper understanding of the physics of molecular interactions at fluid-solid interfaces is key to many emerging applications in material science, chemistry, microengineering, and biology [1]. From a macroscopic point of view, the physics of fluid-solid interactions is conveyed into the specification of appropriate boundary conditions, the common tenet in continuum fluid dynamics being that fluid molecules in the immediate vicinity of a solid wall should move at the same speed of the wall. However, it is well recognized that a variety of fluids do exhibit a net motion relative to the solid wall, a phenomenon known as slip motion [2]. An important measure of slip motion is the slip length,  $l_s$ , defined as the extrapolated distance from the wall where the fluid speed matches exactly the wall speed. The slip length is generally proportional to the molecular mean free path, but for the case of specularly reflecting walls, the constant of proportionality may become so large to generate significant deviations from hydrodynamics in the vicinity of the wall. Since the operation of many micro-devices depends crucially on fluid-wall interactions, it is important to model the effects of a nonzero slip coefficient on the transport properties of such devices. The computational tool of choice to this purpose is molecular dynamics (MD) [3]. However, since MD cannot reach scales beyond a few tens of nanometers, the coupling between MD and fluid models must necessarily proceed through a huge gap in space and time scales. Mesoscopic models are very appealing because they help by reducing this gap considerably.

In this Letter, we present a simple lattice Boltzmann (LB) mesoscopic model to investigate the effects of slip motion on the efficiency of microreactive channels. This mesoscopic model is shown to yield results consistent with previous MD predictions.

The simplest lattice Boltzmann equation (LBE) looks as follows [4,5]:

$$f_i(\mathbf{x} + \delta_i \mathbf{c}_i, t + \delta_t) - f_i(\mathbf{x}, t) = -\omega \delta_t [f_i(\mathbf{x}, t) - f_i^e(\mathbf{x}, t)],$$

where  $f_i(\mathbf{x}, t) \equiv f(\mathbf{x}, \mathbf{v} = \mathbf{c}_i, t)$ ,  $i = 1, n$ , is the probability of finding a particle at lattice site  $\mathbf{x}$  at time  $t$ , moving along the lattice direction defined by the discrete speed  $\mathbf{c}_i$  and  $\delta_t$

is the time unit. The left-hand side of this equation represents the molecular free-streaming, whereas the right-hand side represents molecular collisions via a simple relaxation towards local equilibrium  $f_i^e$  (a local Maxwellian expanded to second order in the fluid speed) in a time lapse of the order of  $\omega^{-1}$ . This relaxation time fixes the fluid kinematic viscosity as  $\nu = c_s^2(\omega - 1/2)$ , where  $c_s$  is the sound speed of the lattice fluid,  $1/\sqrt{3}$  in the present work. In order to recover faithful fluid dynamics, the set of discrete speeds must be chosen such that mass, momentum, and energy conservation are fulfilled. Once this is secured, the fluid density  $\sum_i f_i$ , and speed  $\mathbf{u} = \sum_i f_i \mathbf{c}_i / \rho$  evolve according to the Navier-Stokes equations of fluid dynamics.

In the bulk flow, LBE is essentially an efficient Navier-Stokes solver in disguise. At the solid interface, however, the mesoscopic nature of LBE becomes manifest, because boundary conditions must be imposed on the particle distributions rather than on fluid quantities. For instance, the no-slip boundary condition,  $\vec{u} = 0$ , is typically imposed by reflecting the outgoing populations back into the fluid domain via the so-called bounceback rule. With reference to particles propagating southeast ( $\searrow$ ) from a north-wall boundary placed at  $z = H + 1/2$ , the bounceback rule simply reads  $f_{\searrow}(x, y, H + 1) = f_{\nwarrow}(x + 1, y, H)$  where the lattice spacing is made unity for convenience. This corresponds to a stylized two-body hard-sphere repulsion, with an interaction range equal to  $\sqrt{2}$  lattice units. An interesting generalization of the above rule consists in making allowance for a mix of bounceback and specular reflections:

$$f_{\searrow}(x, y, H + 1) = r f_{\searrow}(x + 1, y, H) + s f_{\nearrow}(x - 1, y, H) \quad (1)$$

where  $r$  is the reflection coefficient and  $s = 1 - r$  is the slip coefficient (see Fig. 1). Note that this is basically a lattice implementation of a physical model of boundary events proposed by Maxwell back in 1879 [6]. Consequently, Eq. (1) cannot aim at any deeper degree of physical realism than Maxwell's model itself. This is in line with the very spirit of the mesoscopic approach: assess the

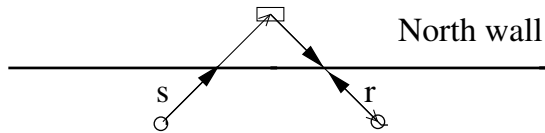


FIG. 1. The schematic mechanism of the slip-boundary conditions between fluid nodes (circles) and boundary nodes (box).

degree of insensitivity of physical observables to the molecular details of the fluid-solid interactions.

As an illustration, we consider a three-dimensional fluid flow in a box of millimetric size. The fluid flow conveys a passive pollutant which, upon hitting the walls of the box, undergoes a first order catalytic reaction of the form  $\frac{dC_w}{dt} = \alpha(C_f - C_w) - \beta C_w$ , where  $C_w$  and  $C_f$  are the pollutant concentration at a solid cell and its fluid neighbor cells, respectively. The coefficients  $\alpha$  and  $\beta$  are empirical inverse time scales for fluid-to-wall mass transfer and catalytic reaction, respectively. This equation is applied to all buffer cells placed at  $z = 0$  and  $z = H + 1$  and serves as a dynamic boundary condition for the pollutant concentration. Note that since flow boundaries are placed halfway between lattice cells, i.e., at  $z = 1/2$  and  $z = H + 1/2$ , the fluid-to-wall mass transfer term  $\alpha(C_f - C_w)$  is correctly evaluated at the boundary of the buffer cells.

The Navier-Stokes equations for the bulk flow are solved by the lattice Boltzmann equation, combined with a customized Lax-Wendroff scheme [7] for the pollutant. The main parameters of the simulation are  $L = 12$  mm,  $H = 3$  mm, and a flow at speed  $U = 10$ – $50$  m/s. On a  $120 \times 30 \times 30$  grid, each lattice spacing corresponds to  $0.1$  mm in size, yielding a lattice time step of about  $0.3 \mu\text{s}$ . The other parameters are (in lattice units) pollutant mass diffusivity,  $D = 0.1$ , fluid kinematic viscosity,  $\nu = 0.01$ , and  $\alpha, \beta$  in the range  $0.001$ – $0.1$ . This yields the following time scales:  $t_D \equiv H^2/D = 9000$ ,  $t_A \equiv L/U = 1200$ , and  $t_W \equiv \alpha^{-1} = 10$ – $1000$ ,  $t_C \equiv \beta^{-1} = 10$ – $1000$ , corresponding to a fast-chemistry scenario in which catalytic processes occur at comparable or shorter scales than fluid advection. Since catalytic processes take place only at the fluid-solid boundary (heterogeneous catalysis), it is of interest to explore the effects of slip motion on the overall efficiency of the catalytic device.

Previous studies [8] suggested that any nonvanishing amount of reflectivity,  $r$ , would ultimately bring the fluid speed at the wall to zero, provided one is willing to wait long enough, namely, of the order of  $t_S \sim e^{ks}$  lattice time units, with  $k$  some constant much larger than unity. This suggestion was backed up by actual calculations in the range  $0.1 < r < 0.5$ , which showed a steep increase of 2 orders of magnitude of the slip relaxation time within the aforementioned range. Since  $r = 0.1$  may still be a relatively large value, in that  $s = 1 - r$  varies by less than a factor of 2 in the range  $[0.1, 0.5]$ , it is natural to wonder whether in the true vicinity of  $r = 0$ , a sort of “glassy” behavior, namely, a nonanalytic blowup of the relaxation

time, would occur. This question is all but academic for nonequilibrium situations, like the reactive, fast microflows explored here, in which all time scales of practical relevance might be much shorter than the slip relaxation time  $t_S$ . It is argued that in the presence of a nonvanishing slip flow (order parameter of the glassy transition) the operational parameters (say, the conversion efficiency) of the device would be significantly affected by slip motion. It is therefore interesting to explore this scenario by a systematic scan in the close vicinity of  $r = 0$ , including the limiting value  $r = 0$ .

Our results indicate that below a critical value  $r < r_c \sim 0.01$  substantial slip motion sets permanently in. By permanently, we mean on time scales significantly longer than the longest fluid-chemical scale in action.

The profiles of the streamwise flow speed at the central chord  $x = L/2$ ,  $y = H/2$  as a function of  $z$  for the sequence of values  $r = 10^{-n}$ ,  $n = 0, 2, 3, 4, 5$ , and  $r = 0$  are shown in Fig. 2. The case  $r = 1$  corresponds to standard parabolic profile (Poiseuille flow) predicted by continuum fluid dynamics. We observe that substantial slip motion sets in for approximately  $r < 0.01$ . The profile on top of the slip layer remains parabolic up to  $r < 0.001$ . For smaller values the shape of the near-wall profile shows a tendency to invert its curvature. These effects can be quantitatively appreciated by plotting the slip length:  $l_s = u_s/u'_w$  as a function of the reflection coefficient  $r$ , where  $u'_w$  is the derivative of the flow profile at the wall (for a Poiseuille flow  $u'_w = 4u_0/H$ ).

This information is shown in Fig. 3, from which we note an exponential inflation of the slip length from scales comparable to the molecular mean free path (straight line at the bottom) all the way up to macroscopic dimensions comparable to the transversal size  $H$  of the fluid domain, covering more than 3 orders of magnitude in the process.

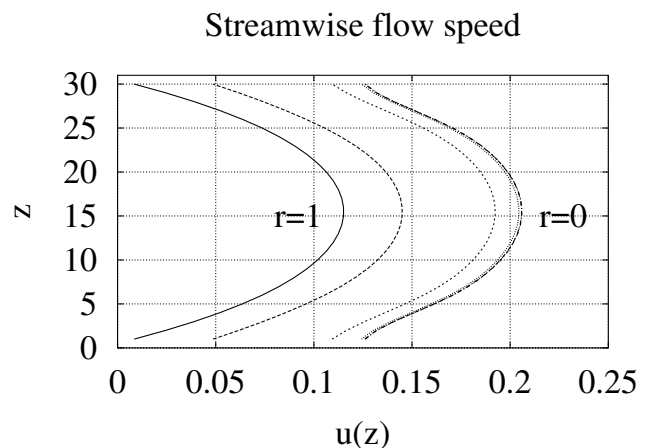


FIG. 2. Streamwise flow speed after 18 000 steps, as a function of cross-flow coordinate  $z$  for different values of the reflection coefficient:  $r = 1, 10^{-2}, 10^{-3}, 10^{-4}, 10^{-5}, 0$  from left to right. The last two curves are indistinguishable at this scale. Here  $\alpha = \beta = 0.01$ .

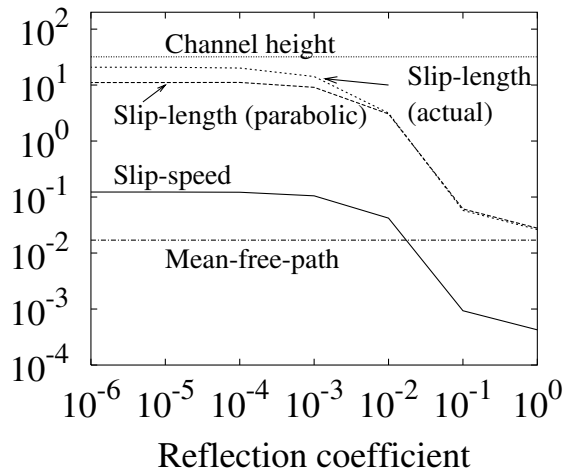


FIG. 3. Slip speed and slip length as a function of the reflection coefficient. Same parameters as Fig. 2.

The extent of the largest slip length, about 20 lattice units (i.e., 20 hard-sphere diameters in molecular language) is interestingly close to results reported by molecular dynamics studies [9]. To be more specific, in Fig. 4 we report the slip length as a function of the pressure gradient  $\nabla p$ , for  $r = 10^{-n}$ ,  $n = 1, 2, 3, 5$ . From this figure we note that, in accordance with MD simulations [9], the slip length grows with decreasing pressure, this effect being particularly spectacular for the case  $r = 10^{-5}$ . Recent molecular dynamics simulations reported a divergent slip length as the shear rate,  $S = U/H$ , approaches a critical value  $S_c$  [10]. Our data do not seem to reproduce such a divergence, which is not surprising since the shear rate in our simulations is about 3 orders of magnitude below  $S_c$ . To make our shear rate comparable with  $S_c$ , LBE should operate on nanometric and picometric space and time scales, respectively, which is clearly beyond the scope and purpose of the mesoscopic approach.

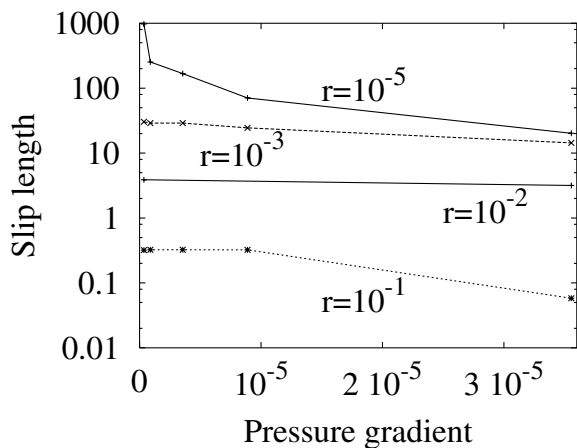


FIG. 4. Slip length as a function of the pressure gradient for  $r = 10^{-n}$ ,  $n = 1, 2, 3, 5$ . The rightmost points correspond to the parameter set of Fig. 2.

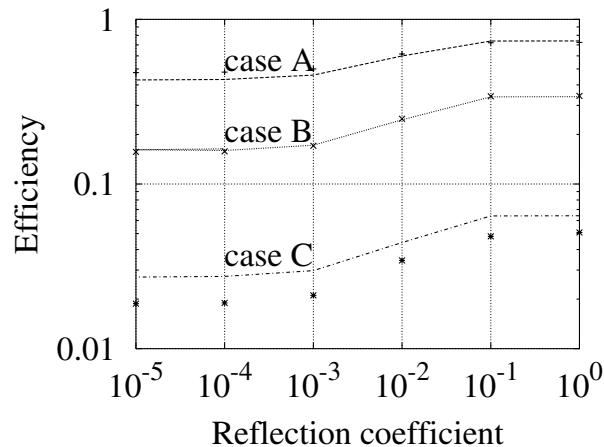


FIG. 5. Conversion efficiency as a function of the reflection coefficient for  $\alpha = \beta = 0.1, 0.01, 0.001$  (A,B,C).

We now consider the effects of slip motion on the conversion efficiency, defined as  $\eta = 1 - \Phi_{out}/\Phi_{in}$ , where  $\Phi_{in}$  and  $\Phi_{out}$  are the fluxes of pollutant at the inlet and outlet sections of the microreactor, respectively. The effects of slip motion on the conversion efficiency are shown in Fig. 5, from which we see that the efficiency is reciprocal to the behavior of the slip length (speed). This can be explained by the following analytical considerations. The conversion efficiency of a smooth microreactive channel can be computed as follows [11]:  $\eta = 1 - e^{-\frac{\chi}{2H} \frac{\lambda(Da)}{Pe}}$  where  $Pe \equiv \frac{UH}{2D}$ , is the Péclet number, measuring advection versus diffusion time scales, and  $Da \equiv \frac{H^2}{4D\tau}$  is the diffusive Damkoehler number measuring diffusion versus chemical time scales (here  $\tau = 1/\alpha + 1/\beta$ ). In the above  $\chi$  is the transversal wave number of the concentration profile, which is obtained by imposing zero speed at the boundary, thus yielding the following algebraic constraint:  $\lambda^2 = \frac{2\delta}{H} Da^2 \cos(\lambda)$  where the lattice spacing  $\delta$  has been reintroduced for the sake of dimensional clarity. The above relation shows that  $\lambda$  is an increasing function of the Damkoehler number. This meets the intuitive notion that high Damkoehler numbers (fast chemistry) associate with high efficiency. Similarly, high Péclet numbers (fast flows) spell poor efficiency, simply because “fast” flows give the pollutant “no time” to react. These qualitative considerations are reflected by quantitative data in Fig. 5, which shows a monotonic drop of efficiency with decreasing values of  $\alpha$  and  $\beta$ . From the above analysis, it is also clear

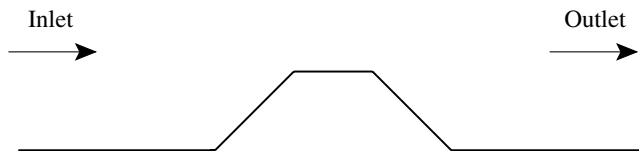


FIG. 6. Detail of the geometry set up for the simulation with a trapezoidal corrugation. A section at  $y = \text{const}$  is shown (out of scale for space reasons).

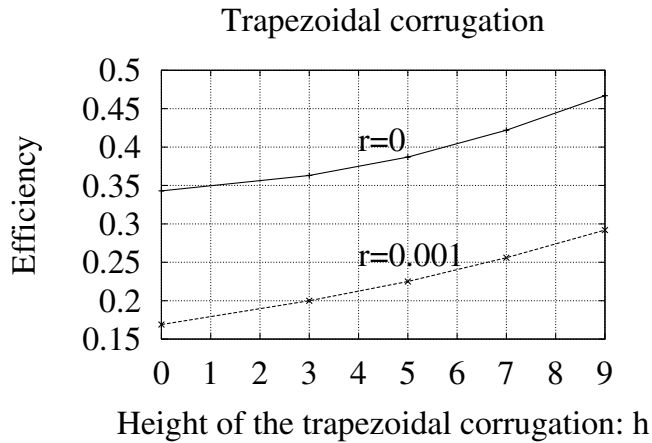


FIG. 7. Conversion efficiency as a function of the height  $h$  of the trapezoidal corrugation, for the cases  $r = 1$  and  $r = 0.001$ . Here  $\alpha = \beta = 0.01$ .

that slip motion can only decrease the overall conversion efficiency of the device. This is again reflected by the results of Fig. 5, which witness a significant deterioration of the conversion efficiency in the region where substantial slip flow is present. This drop in efficiency, measured as  $\eta(0)/\eta(1)$ , yields 0.655, 0.476, 0.372 for cases A, B, C, respectively. Slip-flow results can be interpreted by simply shifting  $u = u + u_s$  in the definition of the Péclet number. The result is reported by the solid lines in Fig. 5, which shows a reasonable agreement with numerical results.

The mesoscopic approach extends naturally to more complex situations where analytical backup is no longer reliable, such as flows with microcorrugations (micro-pumps, valves), which are crucial to the optimal design of microfluidic devices. As a preliminary example of such applications, we have computed the effects on the efficiency of a trapezoidal corrugation of height  $h$  and bases  $b, b + 2h$ , placed in the middle of the bottom wall of the microchannel (see Fig. 6). The trapezoidal corrugation is centered at  $L/2$  with a top base  $b = 10$ , while its height is varied between  $h = 0$  and  $h = 9$ . By deflecting fluid motion, the trapezoidal corrugation promotes a higher cross-flow pollutant transport, which in turn is expected to yield a better efficiency. This effect is reported in Fig. 7, which shows the conversion efficiency as a function of the trapezoidal height  $h$  for the cases  $r = 0$  and  $r = 0.001$ . We observe that a trapezoidal corrugation with  $h = 9$  nearly doubles the conversion efficiency as compared to the smooth channel, almost entirely recovering the deficit due to slip motion. Finally, we point out that results in the high-slip regime are fairly sensitive to the accuracy of

the boundary conditions implementation. For instance, it is readily checked theoretically, and confirmed by numerical simulation, that an apparently minor change to the three-site boundary condition, Eq. (1), such as  $f_{\setminus}(x, y, H + 1) = rf_{\setminus}(x, y, H) + sf_{\nearrow}(x, y, H)$ , results in the complete suppression of slip motion. This shows that boundary conditions for high-slip flows must be handled with care, especially in the presence of geometric irregularities.

In conclusion, we have introduced a mesoscopic lattice Boltzmann model with boundary conditions allowing for slip motion at solid walls. The numerical results show that slip motion degrades the efficiency of microreactive channels, whereas geometrical irregularities have a beneficial effect.

The author thanks the Physics Department of Harvard University for kind hospitality during his stays. He also thanks Professor E. Kaxiras for enlightening discussions.

- 
- [1] G. Whitesides and A. D. Stroock, *Phys. Today* **54**, No. 6, 42 (2001).
  - [2] P. Thompson and M. Robbins, *Science* **250**, 792 (1990); R. Pit, H. Hervet, and L. Léger, *Phys. Rev. Lett.* **85**, 980 (2000); Y. Zhu and S. Granick, *Phys. Rev. Lett.* **87**, 096105 (2001).
  - [3] J. Koplik and J. Banavar, *Annu. Rev. Fluid Mech.* **27**, 257 (1995); J. Koplik, J. Banavar, and I. Willemsen, *Phys Fluids A* **1**, 781 (1989); C. Denniston and M. O. Robbins, *Phys. Rev. Lett.* **87**, 178302 (2001); M. Cieplak, J. Koplik, and J. Banavar, *Phys. Rev. Lett.* **86**, 803 (2001).
  - [4] R. Benzi, S. Succi, and M. Vergassola, *Phys. Rep.* **222**, 145 (1992); S. Chen and G. Doolen, *Annu. Rev. Fluid Mech.* **130**, 329 (1998); S. Succi, *The Lattice Boltzmann Equation* (Oxford University Press, Oxford, 2001).
  - [5] Y. Qian, D. d'Humières, and P. Lallemand, *Europhys. Lett.* **17**, 479 (1992).
  - [6] J.C. Maxwell, *Philos. Trans. R. Soc. 1*, Appendix (1879).
  - [7] S. Succi, H. Chen, C. Teixeira, A. De Maio, and G. Bella, *J. Comput. Phys.* **152**, 493 (1999).
  - [8] P. Lavallée and J. P. Boon, *Physica (Amsterdam)* **47D**, 233 (1991).
  - [9] J.L. Barrat and L. Bocquet, *Phys. Rev. Lett.* **82**, 4671 (1999).
  - [10] P. A. Thompson and S. Troian, *Nature (London)* **389**, 360 (1997).
  - [11] S. Succi, G. Smith, A. Gabrielli, and E. Kaxiras, *Eur. Phys. J. Appl. Phys.* **16**, 71 (2001); S. Succi, G. Smith, and E. Kaxiras, *J. Stat. Phys.* **107**, 343 (2002); S. Succi, O. Filippova, G. Smith, and E. Kaxiras, *Comput. Sci. Eng.* **3**, 26 (2001).